EMMERICHITE, $Ba_2Na(Na,Fe^{2+})_2(Fe^{3+},Mg)Ti_2(Si_2O_7)_2O_2F_2$, A NEW LAMPROPHYLLITE–GROUP MINERAL FROM THE EIFEL VOLCANIC REGION, GERMANY[1]

Nikita V. Chukanov
Institute of Problems of Chemical Physics, Russian Academy of Sciences, Chernogolovka, Russia, chukanov@icp.ac.ru

Ramiza K. Rastsvetaeva
Institute of Crystallography, Russian Academy of Sciences, Moscow, Russia, rast@ns.crys.ras.ru

Sergey M. Aksenov
Institute of Crystallography, Russian Academy of Sciences, Moscow, Russia, aks.crys@gmail.com

Günter Blass
Merzbachstrasse 6, D-52249, Eschweiler, Germany, nc-blaszgu@netcologne.de

Igor V. Pekov
Moscow State University, Geological Faculty, Moscow, Russia, igorpekov@mail.ru

Dmitriy I. Belakovskiy
Fersman Mineralogical Museum, Russian Academy of Sciences, Moscow, Russia, dmz@fmm.ru

Jochen Tschörtner
Judenpfad 40, 50996 Köln, Germany

Willy Schüller
Im Straussenpesch 22, 53518 Adenau, Germany, Willi.Schueller@dlr.rlp.de

Bernd Ternes
Bahnhofstrasse 45, 56727 Mayen, Germany, Bernd.Ternes@dlr.rlp.de

Emmerichite, $Ba_2Na(Na,Fe^{2+})_2(Fe^{3+},Mg)Ti_2(Si_2O7)_2O_2F_2$, a new lamprophyllite-group mineral has been found in the Rother Kopf and Graulay basalt quarries, Eifel volcanic region, Rhineland-Palatinate, Germany in late assemblages consisting of nepheline, augite, melilite, götzenite, lileyite, fluorapatite, as well as (in Rother Kopf) leucite, phlogopite, magnetite, perovskite, and günterblassite. Emmerichite occurs as lamellar crystals up to $0.05 \times 0.3 \times 0.5$ mm in size and epitaxial intergrowths with lileyite. The new mineral is brown, with vitreous luster. It is brittle, the Mohs' hardness is 3−4; cleavage is perfect parallel to {100}. The calculated density is 3.864 g/cm^3. Emmerichite is biaxial, (+), α = 1.725(4), β = 1.728(4), γ = 1.759(4). The chemical composition (electron microprobe Fe^{2+}/Fe^{3+} estimated from X-ray structural analysis, wt.%) is as follows: Na_2O 5.44, K_2O 1.03, CaO 1.98, SrO 3.23, BaO 25.94, MgO 3.13, MnO 2.22, FeO 4.85, Fe_2O_3 6.73, TiO_2 15.21, ZrO_2 0.52, Nb_2O_5 1.32, SiO_2 27.13, F 3.54, -O=F_2 -1.49, total is 100.78. The empirical formula is $Ba_{1.49}Sr_{0.27}K_{0.19}Na_{1.54}Ca_{0.31}Mn_{0.275}Mg_{0.68}Fe^{2+}_{0.59}Fe^{3+}_{0.74}Ti_{1.67}Zr_{0.04}Nb_{0.09}Si_{3.97}O_{16.36}F_{1.64}$. The crystal structure has been refined on a single crystal to R = 0.044. The new mineral is monoclinic $C2/m$, a = 19.960(1), b = 7.098(1), c = 5.4074(3)Å, β = 96.368(1)°, V = 761.37(12)Å^3, Z = 2. Emmerichite is isostructural with other monoclinic minerals of the lamprophyllite group. Its crystal chemical formula is $[Ba,Sr,K]_2[(Na,Ca)(Na,Fe^{2+},Mn^{2+},Mg)_2(Fe^{3+},Mg)][(Ti,Fe^{3+},Nb,Zr)_2(Si_2O_7)_2O_2](F,O)_2$. The strongest lines in the X-ray diffraction pattern [d, Å (I, %) (hkl)]: 9.97 (55) (200); 3.461 (65) (510, 311, 401); 3.312 (40) (220, 600); 2.882 (38) (22-1, 420); 2.792 (100) (221, 511); 2.670 (56) (002, 601, 20-2); 2.629 (45) (710, 42-1); 2.140 (57) (131, 022, 621, 22-2). The type specimen is deposited in the Fersman Mineralogical Museum, Russian Academy of Sciences, Moscow, Russia.
7 tables, 6 figures, 26 references.
Keywords: emmerichite, new mineral, layered titanosilicate, lamprophyllite group, Rotter Kopf, Graulay, Eifel, alkali basalt.

Late pneutomatolitic mineral assemblages related to alkali basalt of the Eifel paleovolcanic region, Rheinland-Pfalz, Germany, are characterized by the wide diversity of mineral species (Blass *et al.*, 2008; 2011) the list of which is expanding every year (Blass *et al.*, 2009_1, 2009_2; 2011; Chukanov *et al.*, 2011_1; 2011_2; 2012_1; 2012_2; 2013). More than ten minerals known from there including titanite, götzenite, fresnoite, fersmanite, batisite, nonkanbachite, lamprophyllite group members (lileyite, fluorine analog of barytolamprophyllite), shüllerite related to the lamprophyllite group, and emmerichite, a new member of this group reported in this paper are titanosilicates.

Emmerichite was named in honor of Franz-Josef Emmerich (b. 1940), German amateur mineralogist and mineral collector for his contributions to the mineralogy of the

[1] — A new mineral species emmerichite and its name approved by the Commission on New Minerals and Mineral Names, Russian Mineralogical Society and by the Commission on New Minerals, Nomenclature, and Classification of Minerals of the International Mineralogical Association (September 2, 2013, IMA no. 2013-064).

Eifel region. In particular, he was initiator and publisher of the first Eifel CD with multiple photos and detailed data on minerals from the Eifel region (Blass *et al.*, 2011).

The type specimen is deposited in the Fersman Mineralogical Museum of the Russian Academy of Sciences, Moscow, Russia; the number in the systematic collection is 94122.

Occurence

Specimens with emmerichite were found in two operating basalt quarries located in the Western Eifel volcanic region, Rheinland-Pfalz, Germany.

The holotype specimen originates from the Rother Kopf Quarry located 20 km WSW of the town Gerolstein near the settlement Roth. In this locality emmerichite occurs as flattened crystals frequently intergrown with altered götzenite and günterblassite (Fig. 1). Associated nepheline, leucite, augite, phlogopite, ekermanite, götzenite, lileyite, fluorapatite, magnetite, and perovskite are pneumatolitic minerals crystallized in cavities within alkali basalt. In some cavities, these minerals are overgrown by late hydrothermal chabasite-K, chabasite-Ca, phillipsite-K, and calcite. Günterblassite is a transformation mineral species formed as a result of partial leaching of cations and anions from the earlier hydrogen-free mineral of the günterblassite group (Chukanov *et al.*, 2012$_2$) that is probably related to umbrianite (Sharygin *et al.*, 2013). Götzenite and ekermanite in this assemblage are usually altered by superimposed hydrothermal processes (up to complete replacement of these minerals with amorphous hydrous silicates).

Cotype specimen of the new mineral was found in the Graulay quarry (other spelling is Graulai, Grauley, Graulei) near the settlement Hillesheim, where the new mineral is associated with nepheline, augite, Ti-rich andradite, titanite, noonkanbahite, lileyite, fresnoite, melilite, götzenite, batiferrite, barite, and late alumohydrocalicite. In this assemblage, emmerichite epitaxially overgrows crystals of lileyite forming rims up to 50 μm in thickness with sharp boundary between these two minerals (Figs. 2, 3).

Morphology and physical properties

Emmerichite occurs as thin lamellar to tabular flattened and occasionally lath-shaped crystals up to 0.05 × 0.3 × 0.5 in size and aggregates of these crystals up to 1 mm across. The major habit form is {100}; {110} and faces of belt {*h*0*l*} are minor. The new mineral is brown of various tints with vitreous luster and white streak. Emmerichite is brittle; the Mohs' hardness is 3−4; the cleavage is perfect parallel to (001). The calculated density is 3.864 g/cm^3.

Emmerichite is biaxial, positive, α = 1.725(4), β = 1.728(4), γ = 1.759(4); $2V_{meas.}$ = 80(5)°, $2V_{calc.}$ = 79°. The dispersion of optical axes is medium, $r > v$. Optical orientation is:

Fig. 1. Lamellar crystals of emmerichite (brown) with günterblassite (colourless) from Rother Kopf. Field of view 1.5 mm. Photo: Volker Betz.
Fig. 2. Emmerichite (dark zones) epitactically overgrowing lileyite crystals from Graulay. Field of view: 0.8 mm. Photo: Fred Kruijen.

$X = a$; the axes Y and Z are parallel to the (100) plane; the axis Y is parallel to the elongation of the crystals. Pleochroism is moderate: Z (brown) ≥ Y (light brown) > X (greenish gray).

The infrared absorption spectrum of emmerichite (Fig. 4) was obtained using an ALPHA FTIR Bruker Optics spectrometer in the range 360 − 3800 cm^{-1} with the resolution of 4 cm^{-1}. The powdered mineral was prepared as a pellet pressed with anhydrous KBr; a similar pure KBr pellet was used as a standard. The wavenumbers of absorption bands in the IR spectrum of emmerichite and their assignment are as follows (cm^{-1}, s − strong, w − weak, and sh − shoulder): 1055sh, 1038s, 954s, 907s, 853s (Si-O stretching vibrations), 686w, 658w (O-Si-O bending vibrations of Si_2O_7 groups), 580sh, 536 (combinations of stretching vibrations of TiO_5 and $Fe^{3+}O_6$ polyhedra), 458s, 400s (combinations of Si-O-Si bending vibrations and stretching vibrations of MO_6, octahedra where M = Fe, Mg, Mn, Ca). The IR spectrum of emmerichite is similar to those of the other minerals of the lamprophyllite group (Fig. 4), especially the

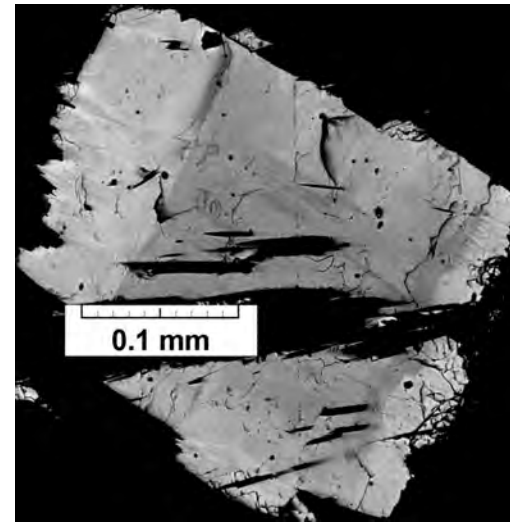

Fig. 3. Back-scattered electron image of emmerichite (light gray zones) with the empirical formula $(Ba_{1.46}Sr_{0.26}K_{0.16}Na_{0.02})_{1.90}Na(Na_{0.60}Fe_{1.10}Mg_{0.76}Mn_{0.27}Ca_{0.27})_{3.00}(Ti_{1.71}Fe_{0.13}Nb_{0.08}Zr_{0.08})_{2.00}(Si_{3.97}Al_{0.03})O_{16.33}F_{1.67}$, *epitaxically overgrowing lileyite (dark gray) with the empirical formula* $(Ba_{1.50}Sr_{0.19}K_{0.19}Na_{0.06})_{1.94}Na(Na_{1.00}Mg_{0.75}Fe_{0.54}Ca_{0.46}Mn_{0.16}Ti_{0.05}Nb_{0.02}Zr_{0.02})_{3.00}Ti_{2.00}Si_{4.00}O_{16.37}F_{1.63}$. *Graulay quarry.*

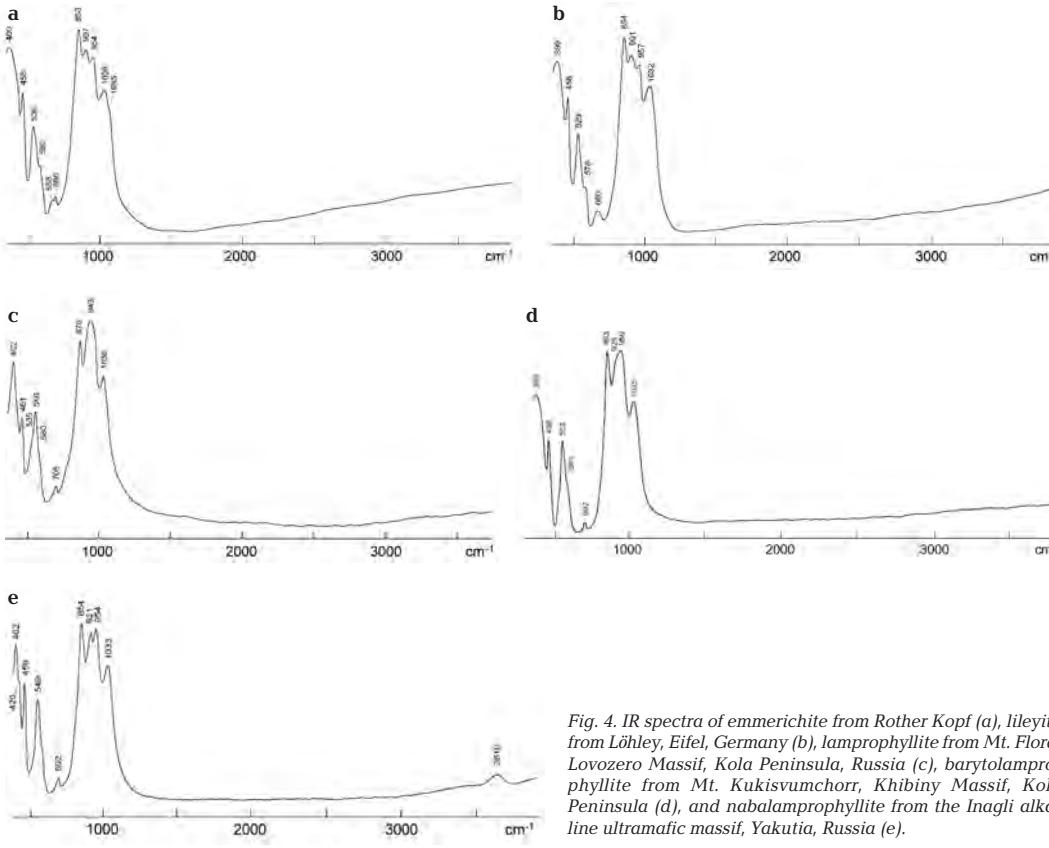

Fig. 4. IR spectra of emmerichite from Rother Kopf (a), lileyite from Löhley, Eifel, Germany (b), lamprophyllite from Mt. Flora, Lovozero Massif, Kola Peninsula, Russia (c), barytolamprophyllite from Mt. Kukisvumchorr, Khibiny Massif, Kola Peninsula (d), and nabalamprophyllite from the Inagli alkaline ultramafic massif, Yakutia, Russia (e).

Table 1. **Chemical composition of emmerichite**

Component	Average content, wt.%	Range of content	Standard
Na_2O	5.44	5.20–5.78	Albite
K_2O	1.03	0.95–1.13	Microcline
CaO	1.98	1.86–2.07	Wollastonite
SrO	3.23	3.02–3.48	SrF_2
BaO	25.94	25.50–26.23	$BaSO_4$
MgO	3.13	3.05–3.28	Diopside
MnO	2.22	2.04–2.43	$MnTiO_3$
FeO*	4.85	10.75–11.16**	Fe_2O_3
Fe_2O_3*	6.73		
TiO_2	15.21	15.05–15.45	$MnTiO_3$
ZrO_2	0.52	0.33–0.78	Zr
Nb_2O_5	1.32	1.04–1.53	Nb
SiO_2	27.13	26.92–27.38	SiO_2
F	3.54	3.35–3.74	CaF_2
O = F	-1.49		
Total	100.78		

*Notes: * – Total iron content (corresponding to 10.91 wt.% FeO) was apportioned between FeO and Fe_2O_3 in the ratio $Fe^{2+}:Fe^{3+}$ = 0.60:0.75 taking into account structural data (cation-ligand distances and bond valence calculations for cationic sites). ** – For total iron considered as FeO.*

Mg-dominant analogue of emmerichite, lileyite, $Ba_2Na(Na,Fe^{2+},Ca)_2(Mg,Fe^{3+})Ti_2(Si_2O_7)_2O_2F_2$ (Chukanov *et al.*, 2012[1]; Fig. 4b). The difference between the two minerals is pronounced in the range 520–690 cm^{-1}. Bands with wavenumbers above 1100 cm^{-1} (that could correspond to stretching vibrations of H-, B- or C-bearing groups) are absent in the IR spectrum of emmerichite.

Chemical composition

The chemical composition of emmerichite was determined using Oxford INCA Wave 700 electron microprobe operated at accelerating voltage 20 kV, current intensity 20 nA, and beam diameter 0.6 μm. Five point analyses were carried out. Average contents of components and ranges of contents are given in Table 1.

The contents of P, S, Al, V, Cr, Ni, Zn, Y, Ln, Th, and U in the mineral are below their detection limits by electron microprobe. Iron was apportioned between Fe^{2+} and Fe^{3+} taking into account structural data (see below). CO_2 and H_2O were not determined. The bands corresponding to H_2O, hydroxyl groups and carbonate anions are absent in the IR spectrum of emmerichite.

The empirical formula of emmerichite calculated on the basis of 18 O+F atoms pfu is $Ba_{1.49}Sr_{0.27}K_{0.19}Na_{1.54}Ca_{0.31}Mn_{0.275}Mg_{0.68}Fe^{2+}_{0.59}Fe^{3+}_{0.74}Ti_{1.67}Zr_{0.04}Nb_{0.09}Si_{3.97}O_{16.36}F_{1.64}$. The simplified formula $Ba_2Na_3Fe^{3+}Ti_2(Si_2O_7)_2O_2F_2$ requires (wt.%) Na_2O 10.31, BaO 34.02, Fe_2O_3 8.86, TiO_2 17.72, SiO_2 26.65, F 4.21, -O = F_2 -1.77, total is 100.00.

X-ray crystallography

The X-ray powder diffraction pattern of emmerichite (Fig. 2) was recorded using a Stoe IPDS II single-crystal diffractometer with an image plate detector, Mo*K*α radiation, an accelerating voltage of 45 kV, and a current of 30 mA. The experiment has been carried out using the Gandolfi method by rotation over two axes (ω and φ), the distance between sample and detector was 200 mm; the measurement time was 40 min. The X-ray powder diffraction pattern of emmerichite is readily indexed in monoclinic unit cell with the following unit cell dimensions refined by the least squares method: a = 19.93(3), b = 7.11(1), c = 5.407(8)Å, β = 96.5(1)°, V = 760(3)Å^3.

Single-crystal X-ray diffraction data were collected with an Xcalibur S CCD diffractometer using Mo*K*α radiation. The monoclinic unit cell dimensions (space group *C*2/*m*) refined from these data are as follows: a = 19.960(1), b = 7.098(1), c = 5.4074(3)Å, β = 96.37(1)°, V = 761.37(1)Å^3, Z = 2.

The crystal structure of emmerichite was solved using 5201 unique reflections with $|F| > 3\sigma(F)$ to R = 0.044. The detailed structural data of emmerichite is reported by Aksenov *et al.* (2014); here only its brief characteristic is given.

The structure of the new mineral (Figs. 5, 6, Tables 3, 4), like the structure of other lamprophyllite-group members, is based on a triple-layered *HOH* packet (module). Inner *O* layer consists of edge-shared octahedra *M*1, *M*2, and *M*3. Outer heteropolyhedral *H* layers are composed of five-coordinated cations polyhedra LO_5 and disilicate groups Si_2O_7. Large cations (Ba, Sr, K) occupy in the space between the packets.

Based on the e_{ref} values, coordination numbers, interatomic distances, character of the distortion of polyhedra, bond-valence calculations and displacement parameters, the occupancy of the sites is:

Ba site – Ba with some Sr and K;

Ti site – Ti with some Fe^{3+}, Nb and Zr;

*M*1 site – Na with subordinate Ca;

*M*2 site – Na with subordinate Fe^{2+}, Mn^{2+} and Mg;

*M*3 site – Fe^{3+} with subordinate Mg;

Table 2. **X-ray powder diffraction data for emmerichite**

$I_{meas.}$	$d_{meas.}$	$I_{calc.}$*	$d_{calc.}$**	*hkl*
55	9.97	39	9.919	200
4	6.68	4	6.683	110
2	4.946	2	4.959	400
2	4.509	3	4.519	201
19	4.119	27	4.114	111
36	3.752	54	3.750	31-1
65	3.461	36, 53, 10	3.463, 3.459, 3.458	510, 311, 401
40	3.312	22, 29	3.341, 3.306	220, 600
27	3.044	45	3.048	51-1
38	2.882	24, 22	2.886, 2.886	22-1, 420
100	2.792	100, 28	2.791, 2.791	221, 511
56	2.670	16, 15, 38	2.687, 2.686, 2.669	002, 601, 20-2
45	2.629	37, 29	2.632, 2.614	710, 42-1
8	2.469	4, 1, 4, 3	2.481, 2.477, 2.466, 2.461	40-2, 421, 71-1, 112
5	2.427	4, 5	2.434, 2.419	31-2, 620
3	2.355	10	2.353	80-1
6	2.269	10	2.272	312
13	2.222	10, 6, 8	2.230, 2.228, 2.209	51-2, 330, 60-2
57	2.140	9, 26, 19, 22	2.142, 2.142, 2.142, 2.133	131, 022, 621, 22-2
15	2.093	16, 6	2.105, 2.086	910, 33-1
28	2.032	8, 22, 4, 13	2.033, 2.032, 2.031, 2.030	42-2, 530, 331, 512
13	1.982	18, 4, 9	1.985, 1.981, 1.961	71-2, 602, 82-1
5	1.934	7, 3	1.937, 1.932	53-1, 10.0.-1
2	1.894	6	1.893	911
3	1.865	8	1.866	531
6	1.813	13	1.816	730
20	1.774	28	1.774	040
8	1.748	5, 3, 3	1.749, 1.748, 1.747	91-2, 11.1.0, 33-2
4	1.715	6, 5	1.717, 1.714	11.1.-1, 113
5	1.654	9, 3, 1	1.658, 1.654, 1.652	51-3, 60-3, 241
4	1.638	7	1.637	313
26	1.601	10, 21, 15	1.604, 1.603, 1.599	22-3, 10.2.1, 023
6	1.560	1, 2, 9	1.563, 1.557, 1.557	640, 71-3, 73-2
2	1.527	2, 4	1.532, 1.523	513, 64-1
27	1.479	24, 8, 4, 3, 2, 17	1.482, 1.481, 1.481, 1.480, 1.479, 1.478	12.2.-1, 042, 641, 423, 13.1.-1, 24-2
5	1.453	11, 2	1.457, 1.452	732, 242
6	1.435	10, 4	1.435, 1.434	93-2, 13-3
6	1.414	3, 2, 2	1.417, 1.415, 1.410	84-1, 133, 10.0.-3
1	1.375	3, 1, 2, 2	1.383, 1.381, 1.372, 1.371	53-3, 803, 841, 333
5	1.354	3, 3, 6	1.356, 1.352, 1.351	11.3.1, 35-1, 20-4
11	1.341	6, 10, 1, 6, 3	1.343, 1.343, 1.337, 1.336, 1.336	004, 12.0.2, 550, 351, 932
6	1.310	2, 5	1.310, 1.309	10.2.-3, 55-1
2	1.291	4, 2	1.287, 1.286	823, 551
2	1.249	2, 2, 2, 2	1.250, 1.249, 1.249, 1.245	71-4, 42-4, 152, 35-2
2	1.224	2, 2	1.223, 1.222	10.4.-2, 13.3.1
3	1.213	1, 1, 3, 2, 3, 1	1.217, 1.215, 1.214, 1.213, 1.211, 1.210	62-4, 55-2, 514, 13.1.-3, 12.2.-3, 64-3
3	1.190	3, 3, 3	1.193, 1.191, 1.189	950, 91-4, 10.2.3
2	1.178	1, 3	1.179, 1.177	552, 16.0.-2
2	1.174	2	1.175	260
2	1.150	2, 2, 2	1.150, 1.150, 1.149	951, 714, 643

Notes: * *— For calculated X-ray pattern, only reflections with intensities ≥ 1 are given.*

** *— Calculated with single-crystal unit cell parameters.*

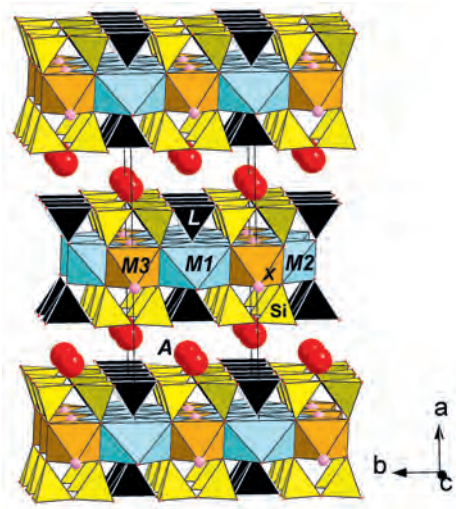

Fig. 5. The crystal structure of emmerichite projected onto (ab) plane.

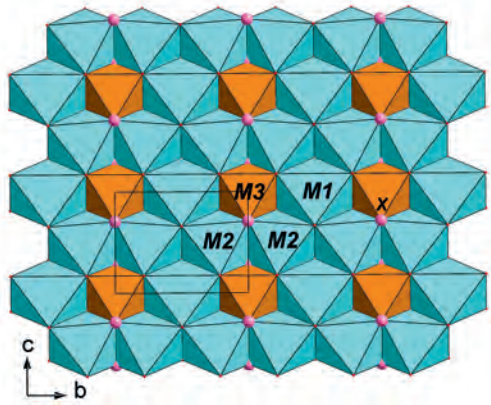

Fig. 6. Octahedral sheet in the structure of emmerichite.

Table 3. **Interatomic distances (Å) in coordination polyhedra of emmerichite**

Ba−O1	2.761(2)	*M*2−O5	2.222(2) ×2
Ba−O3	2.761(2) ×2	*M*2−F	2.283(2) ×2
Ba−O4	2.861(2)	*M*2−O2	2.322(2) ×2
Ba−O4′	2.870(2)	Mean	2.276
Ba−O3′	2.901(2) ×2		
Ba−O1′	2.909(2) ×2		
Mean	2.848		
L−O2	1.703(3)	*M*3−F	2.003(4) ×2
L−O1	1.977(2) ×2	*M*3−O5	2.063(2) ×4
L−O3	1.980(2) ×2	Mean	2.043
Mean	1.923		
*M*1−O2	2.267(3) ×2	Si−O5	1.603(2)
*M*1−O5	2.473(2) ×4	Si−O3	1.624(2)
Mean	2.404	Si−O1	1.627(2)
		Si−O4	1.669(1)
		Mean	1.631

L site − Ti with some Fe^{3+}, Nb, and Zr.

The ions F^- occupy the site at joint of *M*3 octahedron and two *M*2 octahedra.

Discussion

The lamprophyllite group is referred to the bafertisite mero-plesiotype series that in turn belongs to the heterophyllosilicate family (Ferraris *et al.*, 2001; Ferraris, Gula, 2005). The structures of all these minerals are based on triple-layered packet *HOH*, where *O* sheet consists of octahedra MO_6 (*M* = Ti, Nb, Fe^{2+}, Mn^{2+}, Na and other) and *H* is heteropolyhedral sheet composed of tetrahedra SiO_4 (forming groups Si_2O_7) and various six- or five-coordinated high-force-strength cations (Ti, Nb, Zr, Fe^{3+}) (*L*-cations). The general formula of the bafertisite series minerals is $A_2\{M_4[L_2X_{2+p}(Si_2O_7)_2]Y_2\}W$, where *A* are cations with low-force-strength characteristics (as a rule, cations of alkali and alkali-earth elements with coordination numbers higher than 6); *M* are cations of the octahedral sheet, *X* and *Y* are O^{2-}, F^- or OH^-; W are water molecules or polyatomic anions (PO_4^{3-}, SO_4^{2-}, CO_3^{2-}), $p = 0-2$.

In the lamprophyllite group members, *W*-constituents are absent, $p = 0$, the site *Y* is occupied with O^{2-}, and *L*-cations (Fe^{3+} in ericssonite and ferroericssonite or Ti^{4+} in the other members of the group) have the coordination number 5. The general crystal chemical formula of these minerals is $^{[10\text{-}11]}A_2[^{[6]}M1\ ^{[6]}M2_2\ ^{[6]}M3\ X2]\ [^{[5]}L_2(Si_2O_7)_2O_2]$. In Ti-dominant (with Ti at site *L*) members of the group, the octahedra *M*1 and *M*2 are predominantly occupied with Na. Monoclinic minerals (space group *C*2/*m*, the polytype 2*M*) are predominant among studied lamprophyllite-group members. Orthorhombic varieties (space group *Pnmn*, the polytype 2*O*), with the unit cell dimensions varying in the ranges $a = 19.1-20.3$, $b = 7.0-7.1$, $c = 5.3-5.4$Å are known for lamprophyllite, barytolamprophyllite, and ericssonite (Moore, 1971; Matsubara, 1980; Krivovichev *et al.*, 2003; Sokolova, Hawthorne, 2008).

The predominance of Fe^{3+} in the small octahedron *M*3 is the major difference of emmerichite. In the other members of this group, this site is predominated by Ti (in lamprophyllite, barytolamprophyllite, and nabalamprophyllite), Mg (in lileyite), Mn^{2+} (in ericssonite), or Fe^{2+} (in ferroericssonite). In addition to the valence of Fe, emmerichite differs from ferroericssonite in the predominance of Ti in the *L* site and two Na-dominated octa-

Table 4. **Bond valence calculations for emmerichite**

Site	Ba	*L*	*M*1	*M*2	*M*3	Si	V_i
O1	$0.28^{(\times 2)\downarrow}$ $0.28^{\rightarrow}$	$0.65^{(\times 2)\downarrow}$ $0.65^{\rightarrow}$				$1.00^{\downarrow\rightarrow}$	**1.93**
O2		$1.37^{\downarrow}$ $1.37^{\rightarrow}$	$0.27^{(\times 2)\downarrow}$ $0.27^{\rightarrow}$	$0.19^{(\times 2)\downarrow\rightarrow}$			**2.02**
O3	$0.28^{(\times 2)\downarrow}+0.19^{\downarrow}$ $(0.28+0.19)^{\rightarrow}$	$0.64^{(\times 2)\downarrow}$ $0.64^{\rightarrow}$				$1.00^{\downarrow\rightarrow}$	**2.11**
O4	$(0.21+0.21)^{\downarrow}$ $0.21^{(\times 2)\rightarrow}$					$0.89^{\downarrow}$ $0.89^{(\times 2)\rightarrow}$	**2.20**
O5			$0.17^{(\times 4)\downarrow}$ $0.17^{\rightarrow}$	$0.24^{(\times 2)\downarrow}$ $0.24^{\rightarrow}$	$0.40^{(\times 4)\downarrow}$ $0.40^{\rightarrow}$	$1.06^{\downarrow\rightarrow}$	**1.87**
F				$0.21^{(\times 2)\downarrow\rightarrow}$	$0.48^{(\times 2)\downarrow}$ $0.48^{\rightarrow}$		**0.90**
V_i	**1.73**	**3.95**	**1.22**	**1.28**	**2.56***	**3.89**	

Notes: * *— The value* V_i *for M3 site of 2.56 was calculated for the F site occupied by F. In case of O in the F site, corresponding value of* $V_i = 2.56$.

Table 5. **Comparative data for emmerichite and other monoclinic titanium lamprophyllite-group minerals**

Mineral	Emmerichite	Lileyite	Barytolamprophyllite	Lamprophyllite	Nabalamprophyllite
Formula	$Ba_2Na(Na,Fe^{2+})_2(Fe^{3+},Mg)Ti_2(Si_2O_7)_2O_2F_2$	$Ba_2(Na,Fe^{2+},Ca)_3(Mg,Fe^{3+})Ti_2(Si_2O_7)_2O_2F_2$	$Ba_2(Na,Fe^{2+},Mn)_3Ti_3(Si_2O_7)_2O_2(O,OH,F)_2$	$Sr_2(Na,Fe^{2+},Mn)_3Ti_3(Si_2O_7)_2O_2(O,OH,F)_2$	$Ba(Na,Ba)Na_3Ti_3(Si_2O_7)_2O_2(OH)_2$
Space group	*C*2/*m*	*C*2/*m*	*C*2/*m*	*C*2/*m*	*P*2/*m*
a, Å	19.960	19.905	19.833	19.431	19.741
b, Å	7.098	7.098	7.089	7.086	7.105
c, Å	5.407	5.405	5.393	5.392	5.408
β,°	96.37	96.35	96.66	96.75	96.67
Z	2	2	2	2	2
Strong lines of the X-ray powder-diffraction pattern: *d*, Å (*I*, %)	9.97 (55) 3.461 (65) 3.312 (40) 2.792 (100) 2.670 (56) 2.629 (45) 2.140 (57)	3.749 (45) 3.464 (76) 2.792 (100) 2.672 (54) 2.624 (43) 2.140 (52)	3.447 (70) 3.294 (50) 2.801 (100) 2.153 (90) 1.790 (70) 1.601 (80) 1.482 (90)	3.73 (40) 3.43 (55) 3.27 (40) 2.874 (40) 2.773 (100) 2.130 (45) 1.477 (45)	9.87 (96) 3.75 (65) 3.45 (90) 3.275 (78) 3.040 (41) 2.797 (100) 2.610 (43)
Optical data:					
α	1.725	1.718	1.735-1.743	1.733-1.751	1.750
β	1.728	1.735	1.741-1.754	1.740-1.760	1.755
γ	1.759	1.755	1.767-1.778	1.769-1.781	1.799
Optical sign, 2*V*,	+30	+86	+30 — +45	+21 — +43	+40
Density, g/cm^3	3.864	3.776	3.62—3.66	3.44—3.53	3.65
References	This study	Chukanov *et al.*, 2012$_1$	The-Chung Peng, Chien-Hung Chang, 1965; Zhizhong Peng *et al.*, 1984; Rastsvetaeva *et al.*, 1995; Feklichev, 1989	Vlasov *et al.*, 1959; Safyanov *et al.*, 1983; Rastsvetaeva *et al.*, 1990; Feklichev, 1989	Chukanov *et al.*, 2004

hedral sites. The crystal chemical formula of emmerichite is $[Ba,Sr,K]_2[(Na,Ca)(Na,Fe^{2+},Mn^{2+},Mg)_2(Fe^{3+},Mg)][(Ti,Fe^{3+},Nb,Zr)_2(Si_2O_7)_2O_2](F,O)_2$ (interblock cations, cations of the *O* sheet, and the *H* sheet are in brackets).

The unit cell parameters for emmerichite and other monoclinic members of the lamprophyllite group are given in Table 5.

The chemical composition of phyllo- and heterophyllosilicates from pneumatolitic assemblages related to alkali basalt of Eifel — oxyphlogopite $KMg_2Ti(Si_3AlO_{10})O_2$, schüllerite $Ba_2Na(Mn^{2+},Ca)(Fe^{3+},Mg,Fe^{2+})_2Ti_2(Si_2O_7)_2O_2(F,O)_2$, and lamprophyllite group members — are characterized by the absence of hydrogen distinguishing these minerals from their analogues (micas and lamprophyllite group

members) from agpaitic intrusive rocks and pegmatites. Low content of the OH groups is typical also for other primary minerals from the Eifel basalt (amphiboles, fluoraptite, and others). This is evidently caused by the combination of some genetic factors including degassing of magma, high temperature of crystallization and high fugacity of oxygen and fluorine (Chukanov *et al*., 2008).

Acknowledgements

This study has been supported by the Russian Foundation for Basic Research (project no. 14-05-00190-a).

References

Aksenov S.M., Rastsvetaeva R.K., Chukanov N.V. The crystal structure of emmerichite $Ba_2Na_3Fe^{3+}Ti_2(Si_2O_7)_2O_2F_2$, a new lamprophyllite-group mineral // Z. Kristallogr. **2014**. Vol. 229. No. 1.

Blass G., Emmerich F., Graf H.-W., Schäfer Ch., Tschörtner J. Minerale der Eifelvulkane // Version 1.0 / CD. Published by Authors. **2011**. / *URL: http://wannenkopfe.strahlen.org/* (in German).

Blass G., Felsberger-Ruuti S., Kruijen F., Leu K., Locker H., Paulick H., Schmotz F., Schüller W., Ternes B. Die Mineralien der Vulkaneifel // ExtraLapis. **2008**. No. 34. 98 p. (in German).

Blass G., Graf H.-W., Kolitsch U., Sebold D. The new finds from the volcanic Eifel (I) // Mineralien-Welt. **2009$_1$**. Vol. 20. No. 1. P. 46–54 (in German).

Blass G., Graf H.-W., Kolitsch U., Sebold D. The new finds from the volcanic Eifel (II) // Mineralien-Welt. **2009$_2$**. Vol. 20. No. 2. P. 38–49 (in German).

Chukanov N.V., Moiseev M.M., Pekov I.V., Lazebnik K.A., Rastsvetaeva R.K., Zayakina N.V., Ferraris J., Ivaldi G. Nabalamprophyllite, $Ba(Na,Ba)\{Na_3Ti[Ti_2O_2Si_4O_{14}](OH,F)_2\}$, a new layered titanosilicate of the lamprophyllite group from alkaline ultramafic massifs Inagli and Kovdor, Russia // Zapiski VMO. **2004**. Vol. 133. No. 1. P. 59–72 (in Russian).

Chukanov N.V., Mukhanova A.A., Rastsvetaeva R.K., Belakovskiy D.I., Möckel S., Karimova O.V. Britvin S.N., Krivovichev S.V. Oxyphlogopite $K(Mg,Ti,Fe)_3[(Si,Al)_4O_{10}](O,F)_2$, a new mineral species of the mica group // Geol. Ore Deposits. **2011$_1$**. Vol. 53. No. 7. P. 583–590.

Chukanov N.V., Pekov I.V.,Rastsvetaeva R.K., Aksenov S.M., Zadov A.E., Van K.V., Blass G., Schüller W., Ternes B. Lileyite, $Ba_2(Na,Fe,Ca)_3MgTi_2(Si_2O_7)_2O_2F_2$, a new lamprophyllite-group mineral from the Eifel volcanic area, Germany // Eur. J. Mineral. **2012$_1$**. Vol. 24. No. 1. P. 181–188.

Chukanov N.V., Rastsvetaeva R.K., Aksenov S.M., Pekov I.V., Zubkova N.V., Britvin S.N., Belakovskiy D.I,. Schüller W., Ternes B. Günterblassite, $(K,Ca)_{3-x}Fe[(Si,Al)_{13}O_{25}(OH,O)_4]\cdot 7H_2O$, a new mineral: The first phyllosilicate with triple tetrahedral layer // Geol. Ore Deposits. **2012$_2$**. Vol. 54. No. 8. P. 647–655.

Chukanov N.V., Rastsvetaeva R.K., Britvin S.N., Virus A.A., Belakovskiy D.I., Pekov I.V., Aksenov S.M., Ternes B. Schüllerite, $Ba_2Na(Mn,Ca)(Fe^{3+},Mg,Fe^{2+})_2Ti_2(Si_2O_7)_2(O,F)_4$, a new mineral species from the Eifel volcanic district, Germany // Geol. Ore Deposits. **2011$_2$**. Vol. 53. No. 8. P. 767–774.

Chukanov N.V., Rozenberg K.A., Rastsvetaeva R.K., Möckel S. New data on titanium-rich biotite: a problem of "wodanite" // New Data on Minerals. **2008**. Issue 43. P. 72–77.

Chukanov N.V., Zubkova N.V., Pekov I.V., Belakovskiy D.I., Schüller W., Ternes B., Blass G., Pushcharovsky D.Yu. Hillesheimite, $(K,Ca,\square)_2(Mg,Fe,Ca,\square)_2[(Si,Al)_{13}O_{23}(OH)_6](OH)\cdot 8H_2O$, a new phyllosilicate mineral of the günterblassite group // Geol. Ore Deposits. **2013**. Vol. 55. No 7. P. 549–557.

Feklichev V.G. Diagnostic features of minerals. Moscow: Nedra. **1989**. 479 p. (in Russian).

Ferraris G., Gula A. Polysomatic aspects of microporous minerals – heterophyllosilicates, palysepioles and rhodesite-related structures // Rev. Mineral. Geochem. **2005**. Vol. 57. P. 69–104.

Ferraris G., Ivaldi G., Pushcharovsky D.Yu., Zubkova N.V., Pekov I.V. The crystal structure of delindeite, $Ba_2\{(Na,K,\square)_3(Ti,Fe)[Ti_2(O,OH)_4Si_4O_{14}](H_2O,OH)_2\}$, a member of the meroplesiotype bafertisite series // Canad. Mineral. **2001**. Vol. 39. No. 5. P. 1307–1316.

Krivovichev S.V., Armbruster T., Yakovenchuk V.N., Pakhomovsky Ya.A., Men'shikov Yu.P. Crystal structures of lamprophyllite-2*M* and lamprophyllite-2*O* from the Lovozero alkaline massif, Kola peninsula, Russia // Eur. J. Mineral. **2003**. Vol. 15. No. 4. P. 711–718.

Matsubara S. The crystal structure of orthoericssonite // Mineral. J. **1980**. Vol. 10. No. 3. P. 107–121.

Moore P.B. Ericssonite and orthoericssonite. Two new members of the lamprophyllite group from Långban, Sweden // Lithos. **1971**. Vol. 4. P. 137–145.

Rastsvetaeva R.K., Evsyunin V.G., Konev A.A. Crystal structure of K-barytolamprophyllite

// Crystallography Reports. **1995**. Vol. 40. P. 472–474.

Rastsvetaeva R.K., Sokolova M.N., Gusev A.I. Refined crystal structure of lamprophyllite // Mineral. J. **1990**. Vol. 12. No. 5. P. 25–28 (in Russian).

Safyanov Yu.N., Vasilieva N.O., Golovachev V.P., Kuzmin E.A., Belov N.V. Crystal structure of lamprophyllite // Doklady AN SSSR. **1983**. Vol. 269. No. 1. P. 117–120 (in Russian).

Sharygin V.V., Pekov I.V., Zubkova N.V., Khomyakov A.P., Stoppa F., Pushcharovsky D.Yu. Umbrianite, $K_7Na_2Ca_2[Al_3Si_{10}O_{29}]F_2Cl_2$, a new mineral species from melilitolite of the Pian di Celle volcano, Umbria, Italy // Eur. J. Mineral. **2013**. Vol. 25. No. 4. P. 655–669.

Sokolova E., Hawthorne F.C. From structure topology to chemical composition. IV. Titanium silicates: the orthorhombic polytype of nabalamprophyllite from the Lovozero massif, Kola Peninsula, Russia // Can. Mineral. **2008**. Vol. 46. No. 5. P. 1323–1331.

The-Chung Peng, Chien-Hung Chang. New varieties of lamprophyllite-barytolamprophyllite and orthorhombic lamprophyllite // Scientia Sinica. **1965**. Vol. 14. P. 1827–1840.

Vlasov K.A., Kuzmenko M.V., Eskova E.M. The Lovozero alkaline massif. Moscow: AN SSSR. **1959**. 632 p. (in Russian).

Zhizhong Peng, Jianhong Zhang, Jinfu Shu. The crystal structure of barytolamprophyllite // Kexue Tongbao. **1984**. Vol. 29. P. 237–241.